Earth and Planetary Science Letters 579 (2022) 117351

Contents lists available at ScienceDirect

Earth and Planetary Science Letters

www.elsevier.com/locate/epsl

Mantle melting, lithospheric strength and transform fault stability: Insights from the North Atlantic

Fernando Martinez *, Richard Hey

Hawai'i Institute of Geophysics and Planetology, School of Ocean and Earth Science and Technology, University of Hawai'i at Manōa, Honolulu, HI 96822, USA

ARTICLE INFO

Article history:
Received 21 June 2021
Received in revised form 15 December 2021
Accepted 20 December 2021
Available online 13 January 2022
Editor: H. Thybo

Dataset link: https://www.marine-geo.org/tools/entry/MGL1309/

Dataset link: https://dlacruisedata.whoi.edu/AR/cruise/AR35-04/

Dataset link: https://dlacruisedata.whoi.edu/KN/cruise/KN189-04/

Keywords:
transform faults
mantle melting
lithospheric strength
mantle Bouguer anomaly
mid-ocean ridges

ABSTRACT

The offset ridge-transform structure of ocean basins is one of the most prominent expressions of plate tectonics. Yet why this configuration is favored over a continuous divergent boundary has remained unresolved. We examine this issue using mantle Bouguer anomalies (MBAs) from contrasting ridge systems in the North Atlantic. The Reykjanes Ridge north of the Bight transform fault has no transform offsets and is characterized by rapidly propagating melting centers along a linear axis and a continuous MBA low. To the south, the adjoining Mid-Atlantic Ridge has typical ridge segments each underlain by a discrete MBA "bulls-eye" low and offset by transform and non-transform discontinuities. We hypothesize that the pattern of mantle melting, as reflected in the MBAs, creates chemical and rheologic variations in the residual mantle that either favor or hinder transform fault formation. Within ridge segments, mantle melting efficiently extracts water producing dry and strong residual mantle. At segment ends, low extents of melting and inefficient melt extraction preserve damp and weak mantle. On the linear Reykjanes Ridge continuous melting and rapidly propagating melting centers create continuous strong mantle with possibly weak rheologic variations at high angles to the opening direction, not favoring transform faults. In contrast, stable segmented mantle melting on the Mid-Atlantic Ridge forms bands of strong and weak residual mantle aligned in the spreading direction, the latter creating favorable locations for shear deformation and transform faults. Our hypothesis also explains the lack of transform faults at Earth's endmember spreading rates. At ultra-slow ridges, overall melting is limited and irregular and melt extraction is inefficient. At ultra-fast ridges, mantle melting is pervasive and melt extraction is efficient. In both cases, organized spreading-parallel compositional rheological variations do not form and transform faults are not favored. Our model implies that beyond cooling and strengthening with age, the pattern of mantle melting shapes the rheological structure of oceanic lithosphere and the geometry of plate tectonics.

© 2021 Elsevier B.V. All rights reserved.

1. Introduction

Transform faults are strike-slip boundaries where tectonic plates slip horizontally past each other. They connect various convergent and divergent boundaries and together with these boundaries form the geometric elements of plate tectonics (Wilson, 1965). Transform faults most frequently occur between offset seafloor spreading segments where they typically form a single fault or narrow fault zone aligned in the spreading direction with the ridge segments oriented nearly at right angles. Transform faults typically originate after seafloor spreading is established and are not generally inherited from continental rift offsets (Taylor et al., 2009) unless these are quite large (Wilson, 1965). Yet why a segmented and offset ridge-transform pattern is favored over a continuous curvilinear divergent boundary has remained difficult to explain in plate tectonics and geodynamics (Froidevaux, 1973; Püthe and Gerya, 2014; Schierjott et al., 2020; Turcotte, 1974). Further, the entire classes of ultra-slow (Dick et al., 2003) and ultra-fast (Naar and Hey, 1989) ridges, constituting end-member lithospheric thermal structures, characteristically lack transform faults. These observations point to factors beyond lithospheric thermal properties to form and sustain transform faults.

In addition to a gradually thickening thermal lithosphere, seafloor spreading produces rapid and extensive chemical and rheologic changes in the mantle that emerges from the ridge melting regime. In particular, mantle melting removes hydroxyl defects (typically expressed as water content) from olivine, the major constituent of the mantle, thereby increasing the residual mantle viscosity by over two orders of magnitude (Hirth and Kohlstedt, 1996; Phipps Morgan, 1997). This occurs because water behaves as an incompatible element and is strongly partitioned from olivine

* Corresponding author.
E-mail address: fernando@hawaii.edu (F. Martinez).

https://doi.org/10.1016/j.epsl.2021.117351
0012-821X/© 2021 Elsevier B.V. All rights reserved.

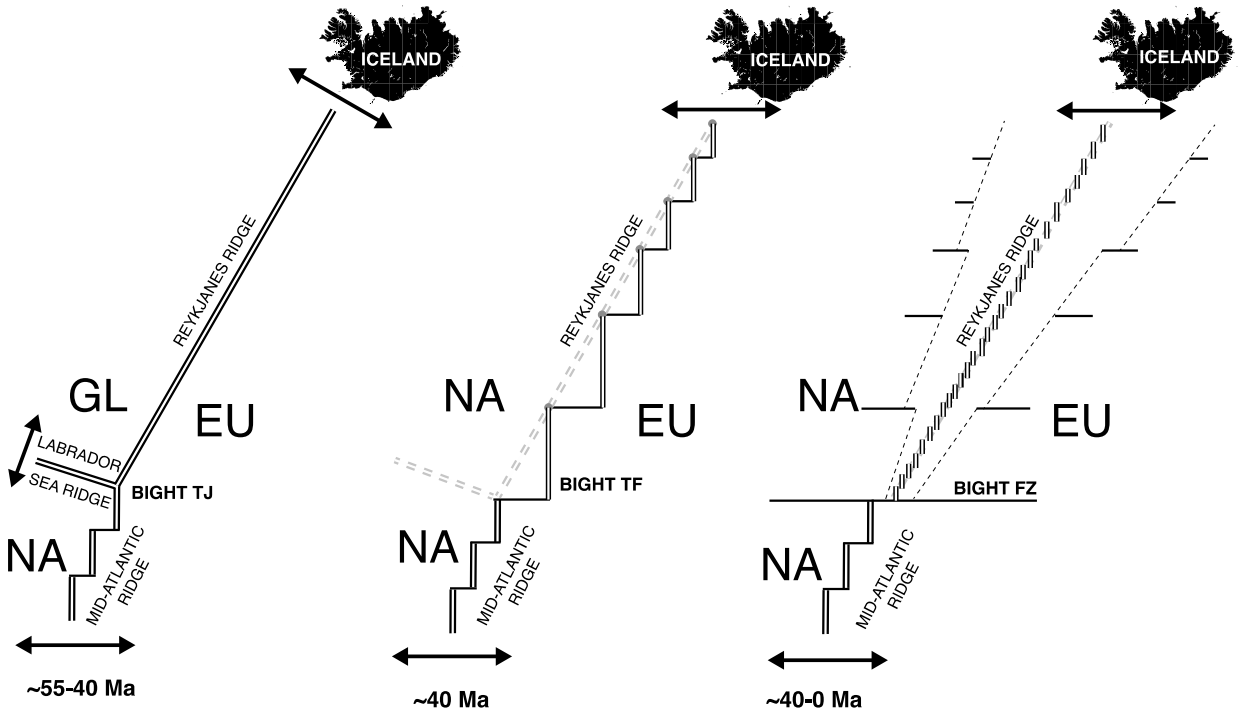

Fig. 1. Schematic depiction of the tectonic evolution of the North Atlantic. Left panel: The early tectonic configuration of the North Atlantic with three plates, Greenland (GL), North America (NA) and Eurasia (EU) separated by three divergent boundaries, the Reykjanes Ridge (GL-EU), Labrador Sea Ridge (NA-GL) and the Mid-Atlantic Ridge (NA-EU) meeting at the Bight triple junction. Double headed arrows depict relative spreading rates and directions. Center panel: After about anomaly 17 (~40 Ma) the Labrador Sea Ridge became extinct, ending the triple junction, joining Greenland to North America and causing a ~30° change in the opening direction of the Reykjanes Ridge. The Reykjanes Ridge became segmented and offset by transform faults in order to spread orthogonally to the new opening direction. The Bight transform fault formed separating the Mid-Atlantic Ridge from the Reykjanes Ridge. Right panel: Promptly after the Reykjanes Ridge became segmented it began to reconfigure back to its original linear configuration from north to south even though this required the ridge to spread obliquely as it became linear again. The Mid-Atlantic Ridge south of the Bight spread ~E-W.

into basaltic melt (Karato, 1986). So, two other important considerations are the extent of melting and the efficiency of melt removal from the mantle. Both may be limited in areas of cool mantle, low mantle upwelling rates and where there is a thick overlying thermal lid—conditions that prevail near ridge segment ends (e.g., Cannat, 1996). On solidifying, hydrous low-degree melts retained in the mantle can reinfuse olivine with hydrogen due the high diffusivity of hydrogen in mantle material (Mackwell and Kohlstedt, 1990). These concepts and observations imply that lithospheric strength should vary as a function of the pattern of mantle melting, both with respect to overall spreading rate and within ridge segments themselves.

Below we apply this hypothesis to the North Atlantic spreading systems, which display contrasting plate boundary geometries and patterns of mantle melting as reflected in their mantle Bouguer anomalies (MBAs), to account for the presence or absence of transform faults on these systems. This hypothesis can be extended generally to account for the occurrence and spacing of transform faults, or their absence, across the global range of spreading rates as the associated patterns of mantle melting vary.

2. Tectonic evolution of the North Atlantic

Following the tectonic rifting of the continental margins of the North Atlantic, several divergent plate boundaries formed at different times (Fig. 1). The Reykjanes Ridge began as the Greenland-Eurasia plate boundary at about anomaly 24 (~55 Ma) in a triple junction configuration with the already existing Mid-Atlantic Ridge (North America-Eurasia plate boundary) and the Labrador Sea spreading center (North America-Greenland plate boundary) (Hey et al., 2016; Fig. 1). The early Reykjanes Ridge spread orthogonally without transform offsets at slow opening rates as a linear axis to about anomaly 17 (~40 Ma) when spreading in the Labrador Sea ceased, joining Greenland to North America, eliminating the triple junction and resulting in a ~30° change in its opening direction (Fig. 1) (Smallwood and White, 2002). This abrupt change in opening direction led to the breakup of the linear Reykjanes Ridge into a series of new segments oriented normal to the new opening direction and offset by transform faults (Fig. 2) (Hey et al., 2016 and references therein). The new segments were roughly centered on the position of the previous axis and the segmentation involved fairly short ridges (<~80 km) and offsets (<~40-45 km) which become less distinct north of about 61°N toward Iceland (Hey et al., 2016) (Fig. 2). The failure of the triple junction also initiated the Bight transform fault (Fig. 1) which has continued to offset the Reykjanes Ridge from the Mid-Atlantic Ridge to the present day (Martinez and Hey, 2017). Despite a stable spreading direction thereafter, as indicated by the linear trend of the Bight fracture zone (Fig. 2), the stair-step ridge-transform configuration of the Reykjanes Ridge was progressively eliminated from north to south (Hey et al., 2016). Magnetic isochrons from the southernmost Reykjanes Ridge indicate that this reconfiguration back to a linear axis was achieved by asymmetric spreading of the offset ridge segments, shortening and finally eliminating the transform offsets (Martinez and Hey, 2017). Such lateral migration of individual segments by asymmetric spreading is not uncommon on the Mid-Atlantic Ridge (e.g., Schouten and White, 1980), however, on the Reykjanes Ridge it proceeded systematically from north to south (Hey et al., 2016; Martinez and Hey, 2017; Martinez et al., 2020).

During the stages when its axis was linear, the Reykjanes Ridge formed southward-pointing V-shaped crustal ridges on its flanks (Fig. 2) (Vogt, 1971). The crustal ridges were originally interpreted as resulting from thermal variations flowing outward from a man-

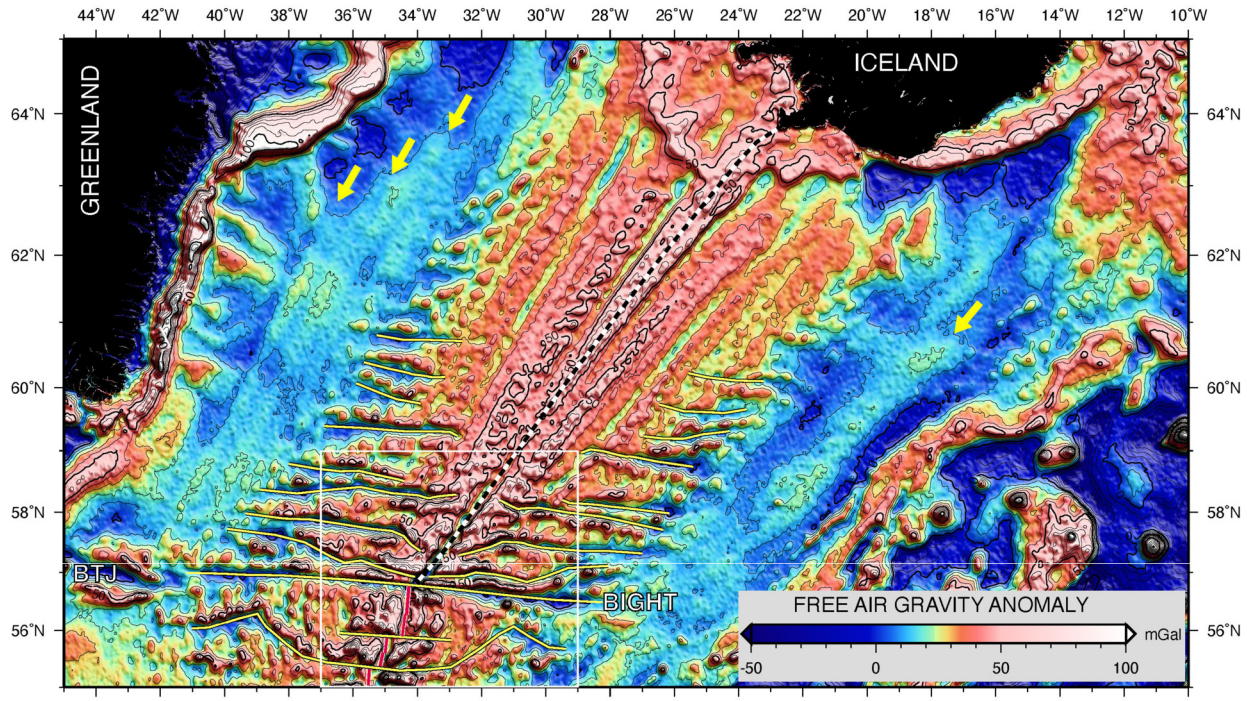

Fig. 2. Regional satellite-derived free-air gravity anomalies in the North Atlantic south of Iceland (Sandwell et al., 2014, v. 30.1). Tectonic features are indicated: Reykjanes Ridge = dashed line; transform faults, fracture zones and non-transform discontinuities = yellow lines; Mid-Atlantic Ridge segments = red lines; BTJ = Bight Triple Junction; Bight transform fault and fracture zone labeled. Yellow arrows indicate interpreted V-shaped crustal ridges in sedimented unsegmented older crust (White, 1997). White box outlines detailed area of Figs. 4–6. (For interpretation of the colors in the figure(s), the reader is referred to the electronic version of this article.)

tle plume beneath Iceland. As the thermal variations migrate along the ridge axis, locally enhanced melting would produce thickened crustal highs that then spread outward onto the ridge flanks to form the V-shaped ridges (Vogt, 1971; White et al., 1995). Other explanations view the troughs bounding the ridges as a type of pseudofault formed by propagating ridge phenomena also responsible for plate-scale crustal accretion asymmetries between North America and Eurasia (Hey et al., 2016). More recent studies interpret the V-shaped ridges as formed by rapidly propagating mantle upwelling instabilities along the ridge axis driven by the large-scale gradient in mantle melting away from Iceland (Martinez and Hey, 2017; Martinez et al., 2020). Whatever process forms them, the V-shaped ridges consist of crustal thickness excesses of about 2 km relative to their bounding troughs (White et al., 1995). Their geometry indicates broad (∼200 km) loci (Searle et al., 1998) of relatively increased mantle melting migrating southward along axis at about 10 times the half spreading rate. There is evidence from regional free air gravity anomalies of V-shaped ridges in the original, now sedimented, crust formed prior to the change in spreading direction when the Reykjanes Ridge was also linear (White, 1997) (Fig. 2). Thus, axially propagating melting centers appear to characterize at least the linear axis stages of the Reykjanes Ridge, and possibly its entire history.

South of the Bight triple junction, which later became the Bight transform fault and fracture zone, the Mid-Atlantic Ridge evolved separately (Fig. 1). The nearly east-west orientation of the Charlie Gibbs fracture zone further south and the subparallel orientation of the Bight fracture zone shows that the Mid-Atlantic Ridge did not undergo large changes in opening direction (Smallwood and White, 2002). The Mid-Atlantic Ridge developed typical transform offsets and NTD's some of which gradually migrated toward and away from Iceland at various times (Fig. 2). V-shaped ridges have not been identified south of the Bight fracture zone, except near the Azores hotspot, and the mode of crustal accretion along the northern Mid-Atlantic Ridge appears like that of other slow-spreading ridges with segmented crust bounded by transform faults and slowly migrating NTDs (Martinez et al., 2020).

3. Mantle Bouguer anomalies

Marine free air gravity variations reflect changes in depth and density of the seafloor and sub-seafloor interfaces and can thus reveal basement structure even in sedimented areas. The free air gravity map of the North Atlantic (Fig. 2) thus images the basement fracture zone and non-transform discontinuity patterns and V-shaped crustal ridges even beneath the sedimented flanks of the Reykjanes Ridge. Removal from the free air gravity anomaly of the effect of the water-crust density contrast and of the crust-mantle density contrast, assuming a uniform thickness crust, yields the mantle Bouguer anomaly (MBA) (Kuo and Forsyth, 1988). Slow spreading ridges typically display focused MBA lows with concentric contours centered near ridge segment mid-points, referred to as "bulls-eye" lows (Kuo and Forsyth, 1988). These anomalies result from departures from the assumed uniform thickness crust as well as unmodeled mantle density variations. Seismic studies (e.g., Dunn et al., 2005; Tolstoy et al., 1993;) confirm that MBA bulls-eye lows result primarily from thicker crust near segment centers relative to segment ends with secondary effects related to lower density in the mantle near segment centers due to higher temperature, melt content and mantle depletion (Lin and Phipps Morgan, 1992). Slow-spreading ridges typically display segmented crust corresponding with discrete bulls-eye MBA lows even when there is little or no offset of the ridge axis. This indicates an active "buoyant" component to mantle upwelling and melting that exists at slow spreading ridges whether or not the plate boundary itself is offset (Lin and Phipps Morgan, 1992). In contrast, fast spreading ridges generally display more uniform crust and MBA lows spanning entire segments, even when these are hundreds of km long (Lin and Phipps Morgan, 1992). The reason for this difference is thought to involve different forms of mantle upwelling between fast- and slow-spreading ridges with two-dimensional pas-

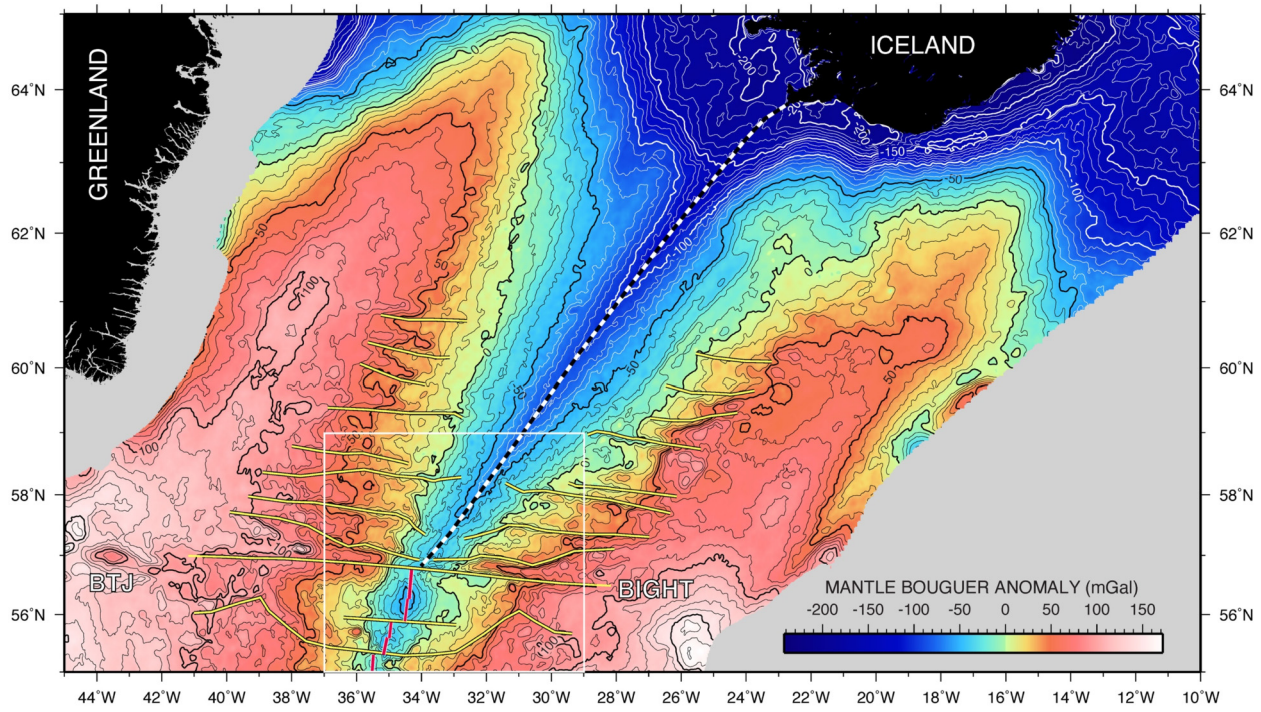

Fig. 3. Regional mantle Bouguer anomaly (MBA) calculated from the satellite-derived free air gravity anomaly and a global bathymetry and sediment thickness database (see Supplementary Information for description of the data sources and processing). Contours are 10 mGals, annotations at 50 mGals. Tectonic features and symbols as in Fig. 2.

sive plate-driven flow at fast ridges and active or buoyant three-dimensional upwelling instabilities at slow ridges (Lin and Phipps Morgan, 1992). Thus, different ridge MBA patterns can be related to different forms of mantle advection and melting, with discrete MBA bulls-eye lows indicating focused three-dimensional cells of mantle upwelling and melting and elongate MBA lows indicating a more continuous two-dimensional pattern of upwelling and melting.

4. Methods

In order to investigate the patterns of mantle upwelling and melting at the Reykjanes and northern Mid-Atlantic Ridges, both slow spreading ridges opening at ~21 mm/yr total rate near the Bight transform fault, we use regional and local data sets to carry out MBA gravity reductions. For the regional analysis we use global bathymetry and sediment thickness databases (see Supplementary Information) and a satellite-derived free air gravity anomaly grid (version 30.1) (Sandwell et al., 2014). The estimated sediment thicknesses are used to account for their gravity effect in flanking areas in the regional data but do not influence our near-axis results where sediment thicknesses are small. The data sets were interpolated in uniform 1 x 0.5 min longitude/latitude grids, which produces roughly equant cell dimensions near 60°N. Following Kuo and Forsyth (1988), densities of 1030 for water, 2730 for basement crust and 3330 kg/m^3 for mantle were assumed. Additionally, we use 2100 kg/m^3 for sediments in off axis areas. We truncated sediment thicknesses less than 100 m to zero to eliminate small, isolated pockets of sediment that had no significant gravity effect. We also tapered isolated sediment patches within ~100 km of the axis to zero. We then increased the seafloor depths by the sediment thicknesses to represent the bottom of the sediment layer. The basement crust was assumed to have a uniform 7 km thickness measured from this surface to yield the Moho (basement/mantle interface) depth. The gravity contributions of the various density interfaces were calculated using five terms in a three-dimensional fast Fourier technique using the GMT program *gravfft* (Wessel et al., 2019) and removed from the satellite-derived free air anomaly values (Fig. 2) to yield the regional MBA anomaly (Fig. 3). Details of the procedure are given in the Supplementary Information.

For the local analysis surrounding the southern end of the Reykjanes Ridge and northern end of the Mid-Atlantic Ridge we primarily used ship multibeam bathymetry (Kongsberg Simrad EM122) from our 2013 R/V Marcus Langseth and 2019 R/V Neil Armstrong cruises, supplemented with available archive multibeam data from the US National Centers for Environmental Information (NCEI) and RRS Charles Darwin cruise CD87 (Searle et al., 1998), available at the Marine Geoscience Data System (MGDS). The multibeam data were cleaned for outliers and gridded at 0.002x0.001 degree spacings in longitude and latitude (roughly 100 m cells) using the global bathymetry database (see Supplementary Information) to interpolate in gaps between swaths with a minimum curvature algorithm in GMT software (Wessel et al., 2019). The resulting bathymetry map is shown in Fig. 4 and reveals details of the basement fabric. For use in gravity reductions this grid was re-interpolated at 1.0 x 0.5 min cell spacings in longitude and latitude, respectively.

For the local gravity analysis, we used primarily ship measurements acquired with Bell BGM-3 gravimeters aboard the R/V Marcus Langseth and R/V Neil Armstrong with satellite-derived gravity used to constrain values more than 5 nautical miles away from the ship data. The combined data were gridded using a minimum curvature algorithm at 1.0 x 0.5 min grid spacings in longitude and latitude, respectively (Fig. 5). MBAs were calculated as above for the regional data but applying no correction for sediments, as basement fabric was evident in most of the multibeam tracks in this near axis setting (Fig. 4). The resulting MBA map is shown in Fig. 6.

5. Results

The MBA maps (Figs. 3 and 6) show contrasting anomaly patterns between the Reykjanes and Mid-Atlantic Ridges separated by the Bight transform fault. North of the Bight, the MBA low is con-

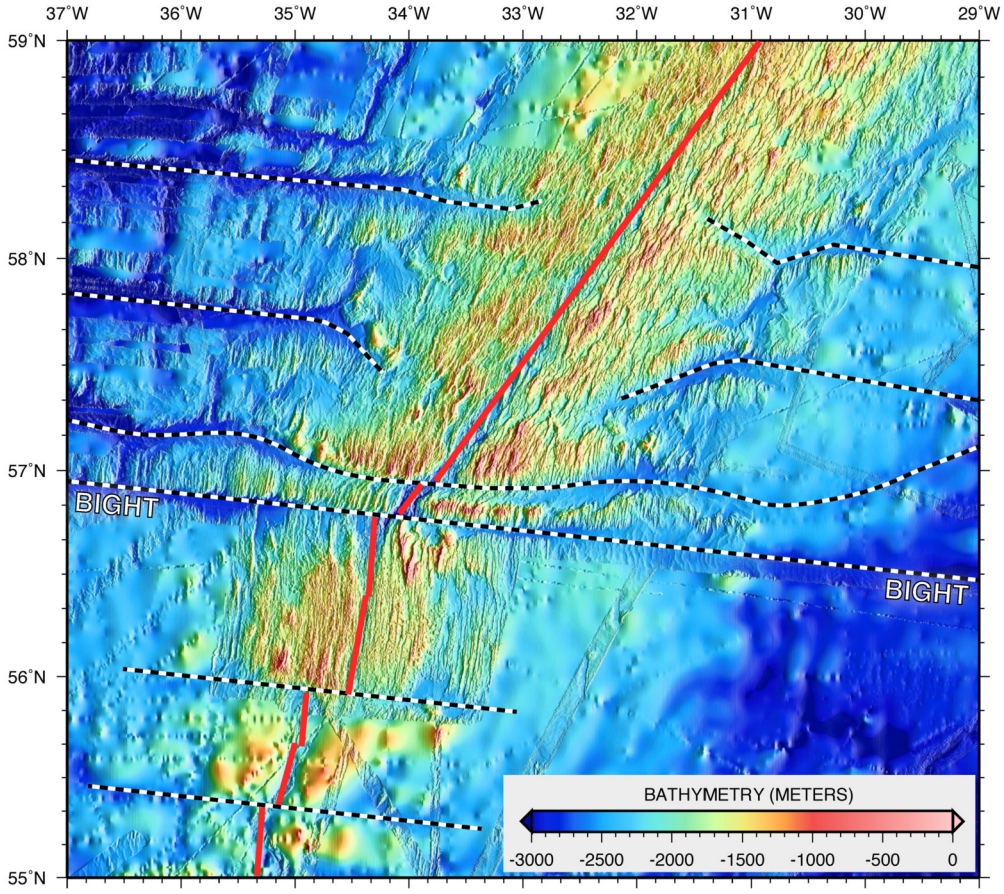

Fig. 4. Detailed bathymetry of the southern end of the Reykjanes Ridge, Bight transform fault/fracture zone (labeled BIGHT) and northernmost Mid-Atlantic Ridge segments. Spreading direction is parallel to the azimuth of the Bight transform fault. Multibeam bathymetry swaths are overlaid on global bathymetry data (see text for data sets used and processing description). Spreading center axes shown as red lines. Transform faults, non-transform discontinuities and fracture zones shown as dashed lines.

tinuous and roughly centered on the Reykjanes Ridge but broadens northward toward Iceland and becomes more negative (Fig. 3). Along the Reykjanes Ridge, seismic studies show that the crust thickens from typical oceanic values (∼7 km) near the Bight transform fault to ∼10-11 km near Iceland (Smallwood et al., 1995; White, 1997) likely contributing most of the negative increase in magnitude of the MBA low towards Iceland (Figs. 3 and 7). The regional along-axis bathymetry and MBA profiles (Fig. 7) extend and confirm earlier results from the detailed RRS Charles Darwin survey showing only low amplitude (<∼5-8 mGal) local MBA variations relative to the axial gradient (Searle et al., 1998). The present intersection of a V-shaped ridge with the axis (Fig. 7), interestingly, does not form a relative low with respect to the linear axial MBA gradient, a finding also shown in Searle et al. (1998). The lack of expression of locally thicker crust in the MBA here may result from compensating dynamic uplift of the Moho boundary as a result of a propagating buoyant instability (Martinez and Hey, 2017). The continuous MBA gradient along the Reykjanes Ridge indicates continuous and thickening crust toward Iceland with no gaps in crust or in mantle melting.

The MBA pattern abruptly changes to the south of the Bight transform fault (Fig. 7). Segments of the Mid-Atlantic Ridge exhibit large (∼35 mGal) bulls-eye lows (Figs. 6 and 7) reflecting thickening crust toward the segment centers. The change in MBAs indicates an abrupt change in the manner of crustal accretion from continuous, gradually thickening crust towards Iceland along the Reykjanes Ridge (White, 1997) to strongly focused loci of crustal accretion on the Mid-Atlantic Ridge (e.g., Dunn et al., 2005; Tolstoy et al., 1993). On the Reykjanes Ridge, the migrating melting centers that produce the flanking V-shaped crustal ridges modulate the already thick crustal thicknesses by about 2 km (White et al., 1995) but do not indicate absence of crust or extremely thin crust within the V-shaped troughs. In contrast, on typical slow-spreading ridges, stable upwelling centers form bulls-eye MBA lows producing spreading-parallel ribbons of thick crust within segment interiors delimited by much thinner or absent crust at segment ends (Kuo and Forsyth, 1988) often exposing mantle material within transform and fracture zone domains (Cannat, 1996; Dick, 1989; Tolstoy et al., 1993). Seismic studies at slow spreading ridges (Dunn et al., 2005; Tolstoy et al., 1993) indicate strongly focused three-dimensional mantle melting near segment centers with limited melting near segment ends. At faster spreading ridges geodynamic studies (Phipps Morgan and Forsyth, 1988; Shen and Forsyth, 1992) indicate that plate-driven passive upwelling, melting and temperatures rapidly diminish within about ±25 km of a large-offset transform fault. The large bulls-eye MBA lows on the northern segments of the Mid-Atlantic Ridge thus indicate focused mantle accretion near segment centers and significantly thinner or absent crust near segment ends.

Free air gravity variations off-axis in the areas of the Reykjanes Ridge fracture zones (Figs. 2 and 5), however, resemble typical patterns associated with oceanic fracture zones suggesting that during the period when transform faults existed on the Reykjanes Ridge, crustal accretion was more focused on the offset segments. It is possible that if the propagating melting centers represent buoyant upwelling instabilities (Martinez and Hey, 2017), they may have continued even during the transform fault stages, within a deep linear "damp" melting regime below the dry solidus (Braun et al., 2000) and beneath the segmented plate boundary. In this case, the lack of evident V-shaped ridges during the transform fault stage

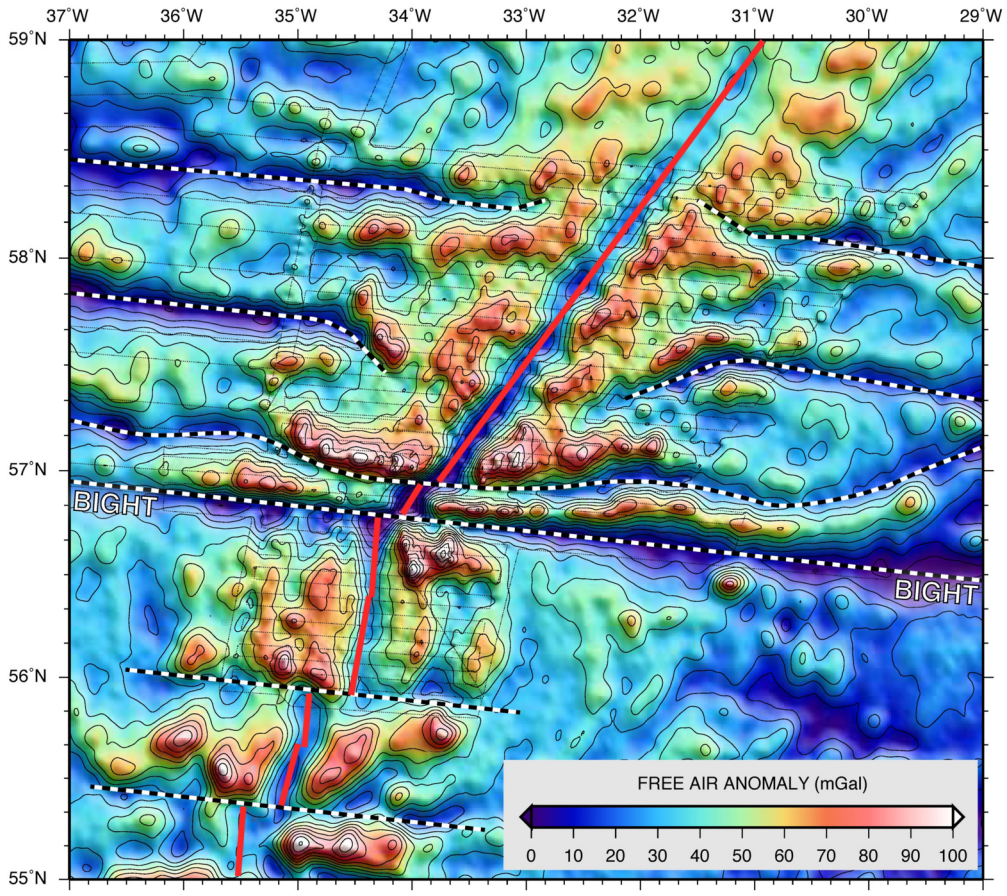

Fig. 5. Ship free air gravity data from R/V Armstrong (AR35-04) and R/V Langseth (MGL1309). Location of ship gravity data is shown as fine dotted lines. Satellite-derived free air gravity data were used beyond 5 nautical miles from ship data. 10 mGal contours shown. See text for data processing. Other symbols as in Fig. 4.

may be explained if mantle melting and crustal accretion are primarily governed by the offset shallow plate boundary, which controls passive plate-driven flow in the more viscous mantle above the dry solidus (Phipps Morgan and Forsyth, 1988). Continued axial propagation of active upwelling instabilities within a deep damp melting interval would have generated a smaller component of melting (Braun et al., 2000), not evident as distinct V-shaped ridges. This could explain why the V-shaped ridges re-formed as the axis became linear. On a linear axis, the shallow plate-driven component of melting is uniform. In this case, only the deeper axially propagating active component of upwelling contributes to forming the V-shaped crustal ridges. Such a separation of passive and active components of ridge mantle flow would appear to be a distinctive if not unique aspect of the Reykjanes Ridge.

6. Discussion

Below we discuss general models of mantle melting and the effect of melting on mantle rheology. We elaborate on how these processes could operate in the context of segmented seafloor spreading systems where melting and melt extraction vary strongly, and discuss implications of recent studies finding basalts and mantle material with elevated water contents near spreading segment ends. We then interpret the contrasting MBA patterns between the Reykjanes Ridge and northern Mid-Atlantic Ridge in terms of differences in the patterns of mantle melting beneath these ridge systems. We infer that the different patterns of melting imply correlated variations in lithospheric rheology and thereby explain the occurrence or absence of transform faults at these seafloor spreading systems. We finally generalize the implications of this hypothesis to explain the occurrence or absence of transform faults across the global range of spreading rates.

6.1. Mantle melting, depletion, melt extraction and water content near ridge segment ends

The spatial form of mantle advection beneath ridges shapes the pattern of melting and the characteristics of the residual mantle (Langmuir et al., 1992; Plank and Langmuir, 1992). Beneath ridge segments, areas where most of the melting occurs are also thought to undergo efficient melt extraction (Langmuir et al., 1992) whereas areas of low extents of melting, as near the deep edges of the melting regime, may trap much of the melt produced (Keller et al., 2017; Plank and Langmuir, 1992). Melt retention may be particularly important near ridge segment ends where slow upwelling rates, cooler mantle and thicker lithosphere are generally predicted (Ligi et al., 2008; Phipps Morgan and Forsyth, 1988; Shen and Forsyth, 1992). Residual mantle is advected away from the melting regime in the spreading direction recording the extents of melting and melt extraction it experienced (Fig. 8). At slow spreading ridges, the degree of depletion of the residual mantle near segment centers is generally thought to be greater than at fast spreading ridges (Plank and Langmuir, 1992) because active upwelling flow is more focused and faster than plate-driven flow (relative to the spreading rate) leading to greater extents of melting. In addition, for discrete active upwelling cells at slow spreading rates, lateral flow of mantle at shallow levels from segment centers along-axis toward segment ends may also suppress upwelling there (Jha et al., 1994) regardless of segment offset. If the melting centers are offset by transform faults the termination of the divergent plate boundary itself will further suppress mantle upwelling increasingly with

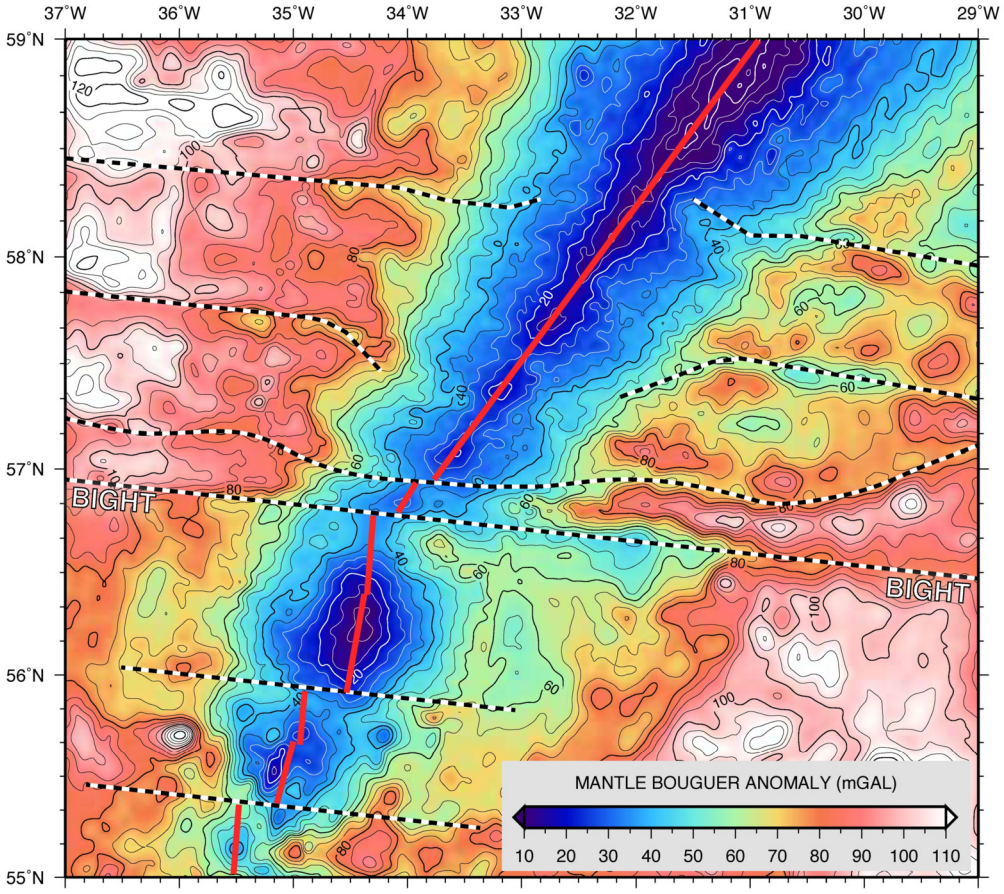

Fig. 6. Mantle Bouguer gravity anomalies obtained using the combined multibeam/regional bathymetry data (Fig. 4) and ship/satellite-derived free air anomaly data (Fig. 5). Data are contoured at 5 mGals with 20 mGal annotations. See text for data processing. Note the elongate mantle Bouguer anomaly low over the Reykjanes Ridge (north of the Bight transform fault) vs. discrete bulls-eye lows over the northern Mid-Atlantic Ridge segments to the south. Other symbols as in Fig. 4.

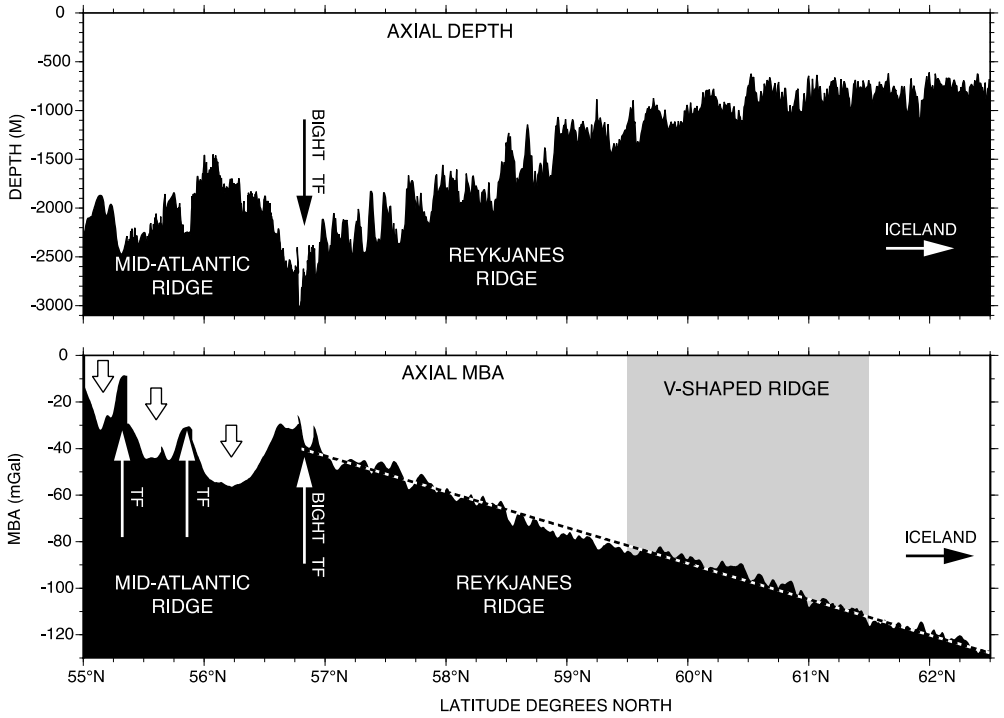

Fig. 7. Axial depth (top) and mantle Bouguer anomaly (MBA) (bottom) along northern Mid-Atlantic Ridge segments and the Reykjanes Ridge south of the volcanic platform surrounding Iceland. The Bight TF (labeled) separates the two ridge systems with contrasting MBA variations. The Reykjanes Ridge exhibits a regional gradient (dashed linear fit) with values decreasing toward Iceland and small amplitude (generally < 8 mGals) local variations whereas the Mid-Atlantic Ridge segments exhibit large (up to ~35 mGal) amplitude MBA bulls-eye lows (outlined arrows; see Fig. 6) between transform faults (TF). The area where a V-shaped ridge intersects the axis is shaded.

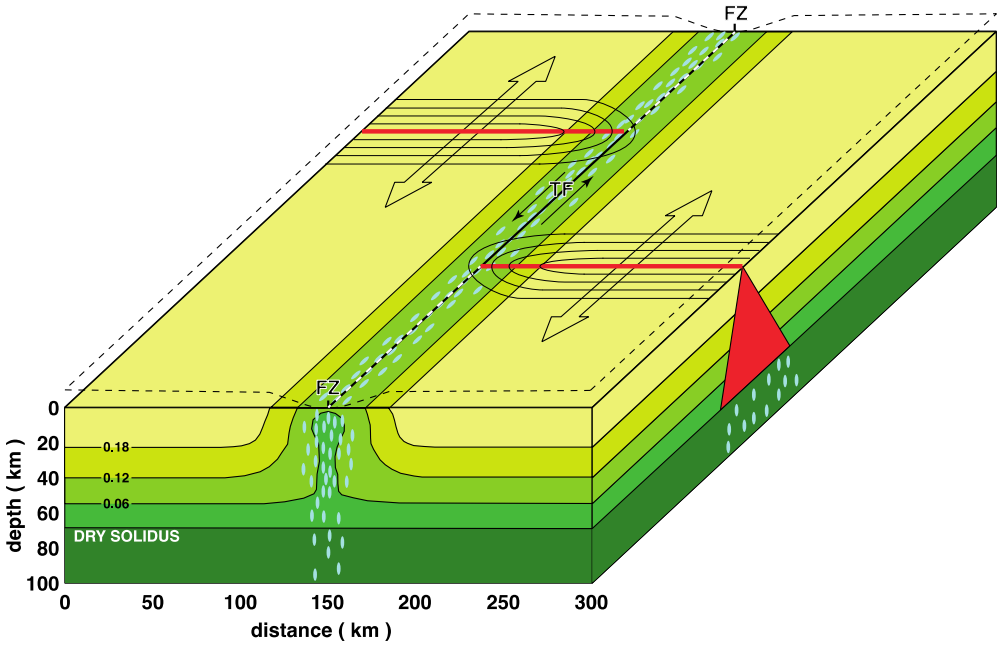

Fig. 8. Three-dimensional depiction of the mantle depletion and melt retention pattern crossing a transform fault (TF) and fracture zone (FZ). Green to yellow colors show contours of fractional mantle depletion for passive mantle flow following Shen and Forsyth (1992) (yellow = most depleted; green = least depleted). Transform fault offsets terminate the divergent plate boundary and suppress mantle upwelling leading to low extents of melting within the mantle near segment ends. Low degree hydrous melts (small blue ovals) formed near segment ends are inefficiently extracted and are frozen in the transform domain mantle. Top solid surface shows intersection of ridges (red lines) with the transform fault (black line) and the fracture zone extensions (dashed). Dashed outlined surface represents the crustal layer showing thinning near the FZ. Large open arrows show spreading direction. Contours on the top mantle surface schematically depict upwelling rates, decreasing away from the ridge axes and toward the transform fault following Shen and Forsyth (1992). Red triangle on right façade depicts the sub-ridge melting regime. Because water is strongly partitioned into melt only residual mantle that did not undergo melting or where melt is inefficiently extracted retains sufficient water to remain weak. Low-degree melts formed beneath the main ridge melting regime mix with shallower higher degree melts and are efficiently extracted to the crust.

offset (Ligi et al., 2008; Phipps Morgan and Forsyth, 1988; Shen and Forsyth, 1992). Therefore, transform offset length is also an important parameter controlling mantle upwelling near segment ends at slow-spreading ridges and is the primary control at fast spreading ridges.

Systematic chemical effects approaching ridge segment ends have long been recognized and termed a “transform fault effect” (Langmuir and Bender, 1984). Chemical effects include increasing incompatible element concentrations, including water, resulting from decreasing extents of melting approaching transform faults. Often basalt and pyroxene samples from near segment ends and from within transform and fracture zone domains show elevated water contents (Gose et al., 2009; Le Roux et al., 2021; Li et al., 2020; Ligi et al., 2005; Schmädicke et al., 2018). Several processes have been suggested to explain the elevated water contents (e.g., Schmädicke et al., 2018; Le Roux et al., 2021). As a general mechanism, however, near segment ends, low degree melting in the deeper “wet melting” portion of the melting interval may be relatively enhanced compared to melting in the shallower dry interval (Ligi et al., 2005) leading to hydrous melts that are not strongly diluted by greater extents of melting as occurs near segment interiors. Such low-degree hydrous melts may become frozen into the relatively cool mantle near segment ends but continue to upwell within the plate-driven solid state mantle flow. Some of these hydrous frozen-in components may thus be eventually exposed at the seafloor near segment ends.

The efficiency of melt removal from the mantle depends on forming an interconnected network of melt at grain boundaries, pores, veins or channels that can convey melt out of the mantle to the crust. This process may be inefficient near the edges of the melting regime (Keller et al., 2017; Plank and Langmuir, 1992) or in general where upwelling rates are low, mantle temperatures are cool and the overlying thermal lithosphere is thick (Cannat, 1996). For example, seismic studies of residual mantle spread from ultra-slow spreading ridges find anomalously low velocities (Conley and Dunn, 2011; Lizarralde et al., 2004) interpreted as a gabbroic component of melt trapped and solidified within the upper mantle. Such conditions of slow upwelling rates, cool mantle and a thick lithospheric lid prevail near segment ends at both slow and fast spreading ridges (Cannat, 1996; Phipps Morgan and Forsyth, 1988; Shen and Forsyth, 1992). Inefficient melt extraction may therefore generally characterize transform fault domains and segment ends. Trapped low-degree melts with high water contents dispersed pervasively within the residual mantle matrix in pores, grain boundaries, veins or meter-scale channels beneath segment ends will rapidly re-infuse surrounding mantle with hydrogen on solidifying due to the high effective diffusivity of hydrogen in mantle material (~10-50 m/My at 1200 °C) (Demouchy, 2010; Le Roux et al., 2021; Mackwell and Kohlstedt, 1990). Thus, both low extents of melting and inefficient melt extraction may combine to preserve hydrous mantle material beneath segment ends.

Despite these general observations and model predictions, some fast-slipping transform faults show only weak crustal thinning or even crustal thickening (Gregg et al., 2007). Geologic observations and melt flow models indicate, however, that volcanism and crustal thickening observed at fast-slipping transforms is primarily due to near-surface processes and is not derived from the mantle beneath the segment ends. Geologic observations indicate that melt may be delivered at shallow levels from the adjacent ridge axes through horizontal dike injection or “overshoot ridges” (Lonsdale, 1986). Geodynamic models also indicate that melt produced within segment interiors may rise vertically and then flow along a shallow lithospheric freezing front or permeable layer to the transform domain (Bai and Montési, 2015; Gregg et al., 2007). Thus, instances of enhanced volcanism and crustal thickness near some fast-slipping transform faults likely do not derive from the imme-

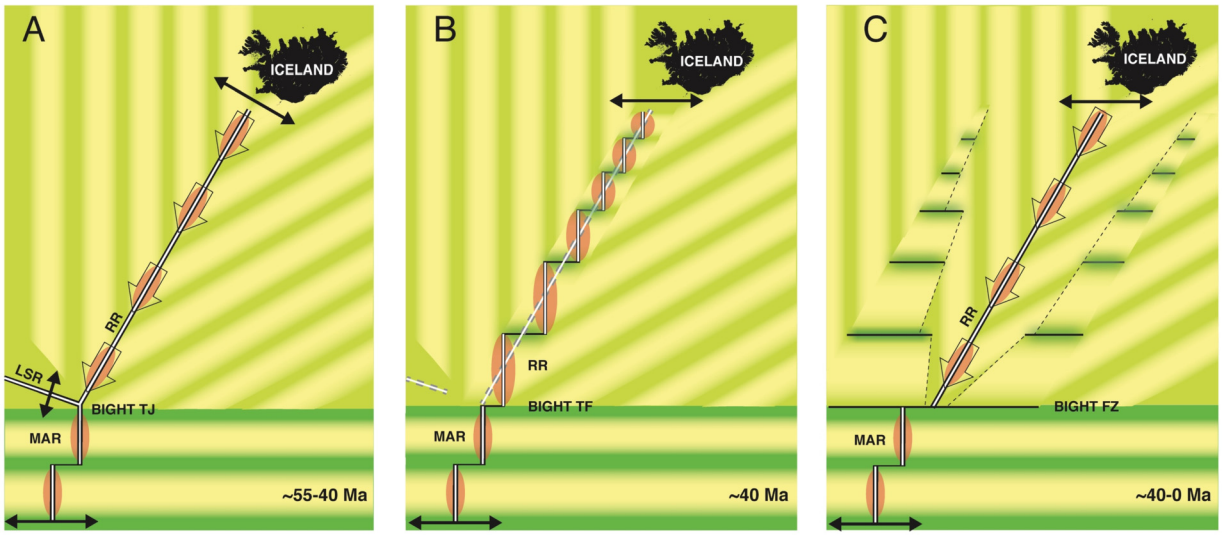

Fig. 9. Schematic illustration of the proposed pattern of mantle depletion, melt extraction, and strength beneath the North Atlantic south of Iceland. Yellower shades indicate mantle with greater depletion, melt removal and strength, whereas greener shades indicate lower depletion, melt removal and strength. (A) The Reykjanes Ridge (RR) originated as an orthogonally spreading linear ridge. Its melting centers (pink ovals) propagated SW along-axis (indicated by open arrows) away from Iceland generating V-shaped crustal ridges and a corresponding but weak pattern of depletion and strength variation in the underlying mantle that was not aligned in the opening direction (double solid arrow) so transform faults were not favored. South of the Bight triple junction the Mid-Atlantic Ridge (MAR) had stable 3-D melting centers indicated by their robust MBAs (see Figs. 3 and 6) generating strong variations in depletion, melt extraction and strength. These rheologic patterns were oriented in the spreading direction favoring transform fault development. When the Labrador Sea Ridge (LSR) failed (B) the RR underwent an abrupt change in opening direction as it became part of the North America-Eurasia plate boundary. An orthogonal ridge-transform plate boundary formed oriented in the opening direction. The transform faults were stable until ridge segment migration removed the offsets and the deep propagating melting centers eliminated the melting patterns formed by the transform faults. (C) The ridge completed its reconfiguration back to its original geometry although now spreading obliquely.

diately underlying mantle but are channeled there by near-surface processes from segment interiors.

An important hypothesis related to mantle melting is that it leads to a pronounced strengthening of the residual mantle due to the removal of water (hydroxyl defects) from olivine since water facilitates various lattice and grain boundary deformation mechanisms in olivine aggregates (Hirth and Kohlstedt, 1996). Water in olivine behaves like an incompatible component on mantle melting with a partitioning coefficient on the order of 10^4 with respect to basaltic melt (Karato, 1986). If melt removal is efficient the water can be removed to the crust yielding a dry residual mantle. These results have been extrapolated generally to the oceanic mantle above the dry solidus to propose an increase in viscosity of over two orders of magnitude in the residual mantle flowing from the ridge melting regime relative to the mantle before melting (Hirth and Kohlstedt, 1996; Phipps Morgan, 1997). Thus, a "compositional" lithosphere extending from the Moho to the dry solidus depth may form close to spreading centers as a result of mantle melting and melt extraction. It has been assumed in these models that because water is strongly partitioned into melt that it is everywhere efficiently removed to the crust to yield a residual oceanic mantle that is uniformly dehydrated and strengthened above the dry solidus. However, as discussed above, the pattern of mantle melting and melt removal beneath segmented ridges is highly variable. If melting near transform domains and segment ends in general is significantly depressed and melt extraction is also inefficient then these areas may preserve significant water content and remain weak. The "compositional" lithosphere may in fact be rheologically segmented mirroring the segmentation of the crust, if not more intensely so, due to shallow redistribution of melt along axis from segment centers toward segment ends as shown by seismic tomographic studies (Dunn et al., 2005) at the Mid-Atlantic Ridge.

6.2. Mantle melting and rheologic variations in the North Atlantic lithosphere

During the linear axis stages of the Reykjanes Ridge, enhanced overall melting due to the Iceland hotspot anomaly would result in a generally depleted mantle (Fig. 9). Any chemical and rheologic variations formed by the axially propagating melting centers would be weak and oriented at high angles to the opening direction. Transform faults would thus not be favored during these times despite oblique spreading during the second linear stage (Fig. 9c). When an abrupt change in opening direction occurred at ~40 Ma, the brittle lithosphere responded mechanically by forming new segments normal to the opening direction offset by transform faults (Fig. 9b). This new plate boundary configuration could have persisted and did last for nearly 40 Myr near the southern Reykjanes Ridge. However, as the segments merged back to their original linear geometry (Martinez and Hey, 2017) transform faults and even non-transform discontinuities disappeared, again replaced by V-shaped ridges (Fig. 9c). The linear Reykjanes Ridge axis today is characterized by only small local MBA gravity variations, typically < 5 mGal (Figs. 3, 6 and 7) (Searle et al., 1998) superimposed on a linear gradient toward Iceland but forming no strongly focused melting centers. In contrast, the divergent plate boundary immediately south of the Bight transform fault evolved separately from the Reykjanes Ridge (Fig. 1) and has stable robust melting centers as indicated by strong local MBA lows $>$ 30 mGal amplitude (Figs. 3, 6 and 7), resulting in the formation of strong crustal segmentation. These crustal patterns imply corresponding variations in residual mantle chemistry, water content and therefore strength oriented in the spreading direction thus favoring transform fault formation and stability at the Mid-Atlantic Ridge (Fig. 9).

6.3. Lack of transform faults at ultra-slow and ultra-fast spreading rates

Our model also explains the general lack of transform faults at the end-member ultra-slow and ultra-fast spreading rates and how

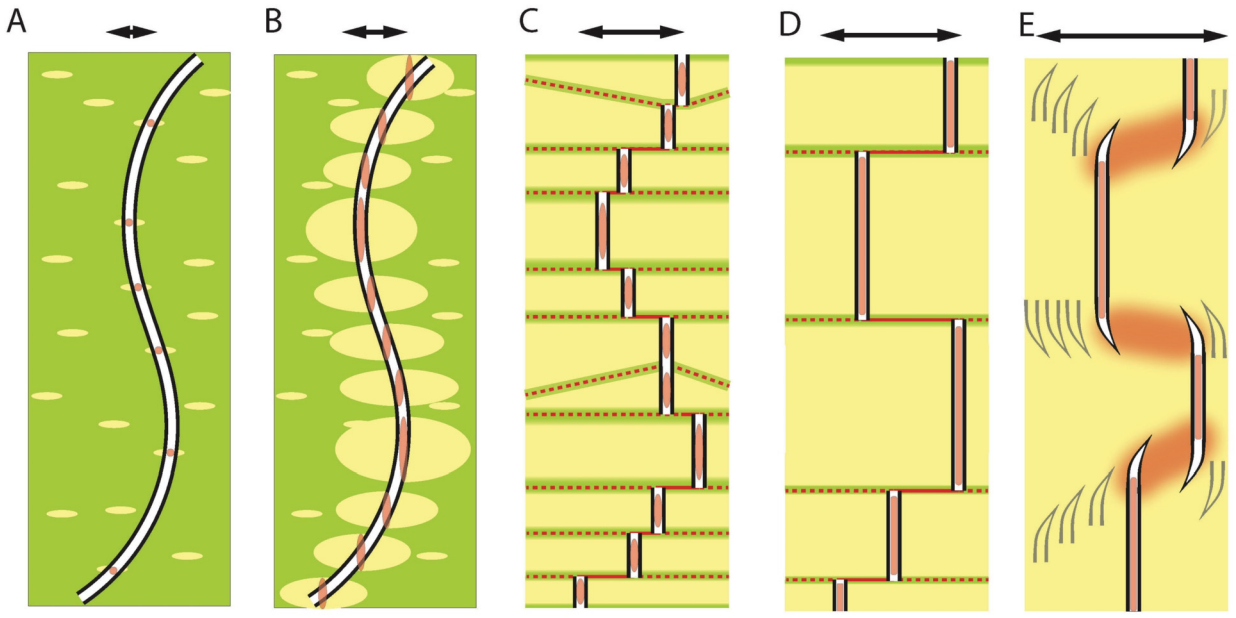

Fig. 10. Model for the evolution of transform faults as a function of spreading rate. Green = damp, weak mantle; yellow = dry, strong, residual mantle. Spreading rates and direction are schematically indicated by length of double arrows at top of panels. Pink ovals are melting centers. (A) Ultra-slow spreading rates (<~20 mm/yr) generate small degrees of overall mantle melting and/or inefficient melt extraction. Volcanic crustal formation is probably limited to especially fertile and irregularly distributed chemical heterogeneities forming local axial volcanic centers generating irregular distributions of strong depleted mantle (small yellow ovals). Despite significant curvature and oblique spreading at some of these ridges, transform faults do not form and a continuous curvilinear divergent boundary is favored. (B) As spreading rates increase, stable 3-D melting centers begin to develop and form corresponding growing zones of depleted (dry, strong) mantle separated by poorly depleted (damp, weak) mantle. (C) At slow spreading rates (>~20 mm/yr), fairly stable 3-D centers of melting generate a banded pattern of strong (yellow) and weak (green) depletion and therefore strength variations in the mantle aligned in the spreading direction allowing transform faults to form (red lines, fracture zones dashed). When ridge offsets are small the melting centers may migrate along-axis due to local mantle heterogeneities forming V-shaped non-transform discontinuities. (D) As spreading rates increase mantle upwelling transitions from buoyant 3-D instabilities to 2-D plate-driven passive patterns where upwelling and melting are rather uniform within segments but depressed at offset segment ends. Thus, transform faults only form at significant offsets of the spreading segments where poorly depleted, damp and weak mantle persists. (E) At ultra-fast spreading centers, the near-axis brittle lithosphere becomes sufficiently weak that overlapping and dueling spreading centers (white ridge tips) form at ridge offsets and generate an effectively diffuse plate boundary zone driving broad and weaker mantle upwelling. Rapid dueling of these overlapping spreading centers results in trails of abandoned tips (grayed out) on the ridge flanks. However, at ultra-fast rates significant mantle melting occurs even in diffuse zones and the mantle is generally depleted forming no weakly depleted bands. Transform fault formation is not favored.

transform fault spacing relates to spreading rate (Fig. 10). At ultra-slow rates (< ~20 mm/yr) mantle melting may be suppressed due to cooling from the surface (Langmuir et al., 1992). Diminished crustal thicknesses observed at ultra-slow spreading rates may also indicate that melt is not efficiently extracted to the crust and remains trapped in the mantle (Cannat, 1996; Conley and Dunn, 2011; Lizarralde et al., 2004) (Fig. 9a). At ultra-slow rates, volcanism occurs as irregularly distributed and variable centers in space and time or as spaced discrete volcanic edifices sometimes forming chains (Dick et al., 2003). This volcanic pattern may reflect irregular mantle chemical heterogeneities where small distributed fertile blobs melt preferentially but overall melting is limited and/or inefficiently extracted. Such spatially and temporally irregular mantle melting does not create magmatically segmented, organized, steady-state spreading-parallel bands of thick and thin crust and corresponding bands of high and low residual mantle depletion, dehydration and strength, so that transform fault formation is not favored (Fig. 10a). Mapping of ultra-slow spreading systems shows that continuous curvilinear divergent boundaries predominate, despite significant spreading obliquity and large changes in trend of the axis, as between the Mohns and Knipovich Ridges. As spreading rates increase, stable cells of mantle melting begin to form as more of the mantle is able to melt. Greater degrees of melting and increasing spreading rates likely also enhance the connectivity of grain boundary melt, porosity, veins and channels and decreases the axial thermal lithospheric thickness so that melt is more efficiently extracted to the crust (Fig. 10b). This begins to form a stable segmented crustal and residual mantle rheological structure aligned in the spreading direction. Oblique spreading and changes in trend are mechanically better accommodated by stair-step ridge-transform offset segments following the strong/weak rheologic variations rather than a continuous curvilinear boundary (Fig. 10b-c). By slow-spreading rates (~20-50 mm/yr), fairly stable mantle melting centers predominate generating a systematic strong and weak banded rheological structure in the underlying mantle, thus favoring stable transform faults (Fig. 10c). At slow spreading rates, mantle upwelling instabilities form at preferred spacings of ~40-80 km (Lin and Phipps Morgan, 1992), thus transform faults also generally have this spacing. As spreading rates increase to fast rates (Fig. 10d) mantle upwelling, melting and the corresponding rheological patterns become two-dimensional—determined by the plate boundary geometry rather than buoyant instability spacing (Lin and Phipps Morgan, 1992). Thus, as rates increase, transform faults can only form at larger ridge axis offsets where the termination of the divergent plate boundary suppresses mantle upwelling and melting (Fig. 10d). At ultra-fast rates (>~145 mm/yr) transform faults are no longer observed (Naar and Hey, 1989). Although at ultra-fast rates a general near-axis weakening of the thermal lithosphere may occur promoting overlapping and dueling spreading tips (Naar and Hey, 1989), these distributed zones of extension still create significant upwelling and melting at ultra-fast rates so that melting and efficient melt extraction is ubiquitous. Thus, no systematic weak rheological bands are produced and transform faults are again not favored (Fig. 10e).

Rapid changes in plate opening direction can still initiate new transform faults in the brittle upper lithosphere even without a pre-existing rheological structure or even cross cutting such a structure, as we infer occurred on the Reykjanes Ridge (Figs. 1 and 9b). In other places where such rapid changes in spreading direction have formed new sets of transform faults, as in the Parece

Vela basin, they appear to be stable even when ridge offsets are small. This is probably because the melting centers are also stable due to a relatively uniform mantle composition. However, the example of the Reykjanes Ridge suggests that when offsets are small or become small, regional gradients in mantle melting properties (as with distance to the Iceland hotspot) can cause melting centers to migrate (Martinez et al., 2020) removing transform faults and even non-transform discontinuities.

The rheological mantle structure created by stable melting centers can also explain the origin of oceanic transform faults following continental rifting even when there are no significant preexisting offsets of the continental margin (Taylor et al., 2009). Only after oceanic spreading begins can mantle melting form the segmented spreading-parallel rheological structure favoring transform fault formation. If the breakup boundary is oblique to the spreading direction and spaced stable melting centers form, a stair-step orthogonal ridge transform geometry will likely form. If early mantle melting is excessive, however, as at volcanic passive margins, then the residual mantle will be generally depleted and dehydrated without weak rheologic bands leading to the formation of continuous linear or curvilinear early seafloor spreading centers, as occur bordering the volcanic passive margin sections of the North Atlantic.

Geodynamic models of ridge segmentation that include only thermal and melt controlled rheologic variations use a priori weaknesses "seeded" in the model domain to generate transform and non-transform offsets and often create highly asymmetric spreading and curved ridge segments (e.g., Püthe and Gerya, 2014). Geodynamic studies also suggest that transform faults modeled primarily as lithospheric mechanical boundaries tend to be short lived—stable for only ~2 Myr, without further rheological weakening within the deeper mantle (Schierjott et al., 2020). The compositionally based rheologic variations proposed here are naturally formed by the segmented nature of mantle melting at seafloor spreading centers: Strong domains form beginning near the ridge axis within segment interiors and extend from the Moho to the dry solidus depth. Weak domains form at segment ends due to low extents of melting, melt retention and local re-fertilization of mantle with hydrogen from these hydrous melts on solidifying. These processes likely provide the additional physical mechanisms needed to stabilize the typically orthogonal and symmetric ridge-transform structure of divergent plate boundaries. Although geodynamic models have yet to incorporate such complex and dynamic effects, they are strongly implied by empirical observations of MBA patterns, supported by seismic, geologic, and geochemical studies confirming the correlated patterns of mantle melting. Our hypothesis proposes a predominant control of mantle melting in generating the segmented character of oceanic plate tectonics by creating a dynamic compositional control on lithospheric rheology. Melting centers grow, shrink and migrate in response to heterogeneities in mantle composition and in response to their own dynamics and with their evolution shape lithospheric rheology and the geometry of plate tectonics.

7. Conclusions

Mantle Bouguer anomalies in the North Atlantic indicate different patterns of mantle melting between the Reykjanes Ridge and northern Mid-Atlantic Ridge. We propose that the pattern of mantle melting shapes the chemical and rheologic structure of the residual mantle, either favoring or inhibiting the formation of transform faults on these systems. Melting within segment interiors efficiently removes water creating a dry and strong residual mantle lithosphere whereas low extents of melting and inefficient melt removal at segment ends preserves damp and weak residual mantle. Where melting centers are stable, as on the Mid-Atlantic Ridge, strong and weak rheological bands are generated in the spreading direction corresponding to segment centers and ends respectively. The weak zones favor the formation of shear zones between the strong bands and therefore favor transform faults. Where melting is pervasive or where melting centers rapidly migrate, as on the Reykjanes Ridge, residual mantle will be generally strong and only weak rheological bands may form but at an angle to the spreading direction, not favoring transform faults. This concept may be extended to the full range of spreading rates explaining the general lack of transform faults at ultra-slow and at ultra-fast rates. At these endmember rates melting and/or melt extraction is either limited or ubiquitous so that systematic rheological bands do not form and transform faults are not favored. Our hypothesis implies a more complex rheological structure to the oceanic lithosphere than suggested by purely thermal controls on strength or models that consider rather uniform mantle dehydration above the solidus depth. It explains the existence, spacing and persistence of transform faults, or their absence, over the full range of seafloor spreading rates as a function of the associated patterns of mantle melting.

CRediT authorship contribution statement

The authors are co-investigators on the research projects. FM wrote the initial draft and both authors collaborated on the interpretations and revisions.

Declaration of competing interest

The authors declare that they have no known competing financial interests or personal relationships that could have appeared to influence the work reported in this paper.

Data availability

Regional databases are available through the referenced sites and original ship data are publicly available at the following databases:
https://www.marine-geo.org/tools/entry/MGL1309/
https://dlacruisedata.whoi.edu/AR/cruise/AR35-04/
https://dlacruisedata.whoi.edu/KN/cruise/KN189-04/

Acknowledgements

This work was funded by NSF grants OCE-1756760, OCE-0452132 and OCE-1154071. We thank the governments of Iceland and Greenland for permission to work in their foreign clearance areas and the Captains, crews and science parties of the R/Vs *Knorr* (KN189-04), *Marcus G. Langseth* (MGL1309) and *Neil Armstrong* (AR35-04) for their support. We thank Ármann Höskuldsson and the University of Iceland for their collaboration on the research cruises, Deborah Eason for comments on an earlier draft and three anonymous reviewers for their detailed constructive comments, which improved the manuscript. SOEST contribution #1454 and HIGP contribution #2456.

Appendix A. Supplementary material

Supplementary material related to this article can be found online at https://doi.org/10.1016/j.epsl.2021.117351. These data include Google maps of the described in this article.

References

Bai, H., Montési, L.G., 2015. Slip-rate-dependent melt extraction at oceanic transform faults. Geochem. Geophys. Geosyst. 16 (2), 401–419.

Braun, M.G., Hirth, G., Parmentier, E.M., 2000. The effects of deep damp melting on mantle flow and melt generation beneath mid-ocean ridges. Earth Planet. Sci. Lett. 176 (3–4), 339–356.
Cannat, M., 1996. How thick is the magmatic crust at slow spreading oceanic ridges? J. Geophys. Res., Solid Earth 101, 2847–2857.
Conley, M.M., Dunn, R.A., 2011. Seismic shear wave structure of the uppermost mantle beneath the Mohns Ridge. Geochem. Geophys. Geosyst. 12 (10).
Demouchy, S., 2010. Diffusion of hydrogen in olivine grain boundaries and implications for the survival of water-rich zones in the Earth's mantle. Earth Planet. Sci. Lett. 295 (1), 305–313. https://doi.org/10.1016/j.epsl.2010.04.019.
Dick, H.J.B., 1989. Abyssal peridotites, very slow spreading ridges and ocean ridge magmatism. Geol. Soc. (Lond.) Spec. Publ. 42 (1), 71–105. https://doi.org/10.1144/gsl.sp.1989.042.01.06.
Dick, H.J.B., Lin, J., Schouten, H., 2003. An ultraslow-spreading class of ocean ridge. Nature 426 (6965), 405–412.
Dunn, R.A., Lekić, V., Detrick, R.S., Toomey, D.R., 2005. Three-dimensional seismic structure of the Mid-Atlantic Ridge (35°N): evidence for focused melt supply and lower crustal dike injection. J. Geophys. Res., Solid Earth 110. https://doi.org/10.1029/2004JB003473.
Froidevaux, C., 1973. Energy dissipation and geometric structure at spreading plate boundaries. Earth Planet. Sci. Lett. 20 (3), 419–424. https://doi.org/10.1016/0012-821X(73)90020-4.
Gose, J., Schmädicke, E., Beran, A., 2009. Water in enstatite from Mid-Atlantic Ridge peridotite: Evidence for the water content of suboceanic mantle? Geology 37 (6), 543–546.
Gregg, P.M., Lin, J., Behn, M.D., Montési, L.G., 2007. Spreading rate dependence of gravity anomalies along oceanic transform faults. Nature 448 (7150), 183–187.
Hey, R., Martinez, F., Höskuldsson, Á., Eason, D.E., Sleeper, J.D., Thordarson, S., Benediktsdóttir, Á., Merkuryev, S., 2016. Multibeam investigation of the active North Atlantic plate boundary reorganization tip. Earth Planet. Sci. Lett. 435, 115–123. https://doi.org/10.1016/j.epsl.2015.1012.1019.
Hirth, G., Kohlstedt, D.L., 1996. Water in the oceanic upper mantle: implications for rheology, melt extraction and the evolution of the lithosphere. Earth Planet. Sci. Lett. 144, 93–108.
Jha, K., Parmentier, E.M., Phipps Morgan, J., 1994. The role of mantle-depletion and melt-retention buoyancy in spreading-center segmentation. Earth Planet. Sci. Lett. 125 (1–4), 221–234.
Karato, S., 1986. Does partial melting reduce the creep strength of the upper mantle? Nature 319 (6051), 309–310.
Keller, T., Katz, R.F., Hirschmann, M.M., 2017. Volatiles beneath mid-ocean ridges: Deep melting, channelised transport, focusing, and metasomatism. Earth Planet. Sci. Lett. 464, 55–68.
Kuo, B.-Y., Forsyth, D.W., 1988. Gravity anomalies of the ridge-transform system in the south Atlantic between 31 and 34.5°S: upwelling centers and variations in crustal thickness. Mar. Geophys. Res. 10 (3–4), 205–232.
Langmuir, C.H., Bender, J.F., 1984. The geochemistry of oceanic basalts in the vicinity of transform faults: observations and implications. Earth Planet. Sci. Lett. 69, 107–127.
Langmuir, C.H., Klein, E.M., Plank, T., 1992. Petrological systematics of mid-ocean ridge basalts: constraints on melt generation beneath ocean ridges. In: Phipps Morgan, J., Blackman, D.K., Sinton, J.M. (Eds.), Mantle Flow and Melt Generation at Mid-Ocean Ridges. American Geophysical Union, Washington, DC, pp. 183–280.
Le Roux, V., Urann, B.M., Brunelli, D., Bonatti, E., Cipriani, A., Demouchy, S., Monteleone, B.D., 2021. Postmelting hydrogen enrichment in the oceanic lithosphere. Sci. Adv. 7 (24). https://doi.org/10.1126/sciadv.abf6071.
Li, P., Xia, Q.-K., Dallai, L., Bonatti, E., Brunelli, D., Cipriani, A., Ligi, M., 2020. High H_2O content in pyroxenes of residual mantle peridotites at a Mid Atlantic Ridge segment. Sci. Rep. 10 (1), 579. https://doi.org/10.1038/s41598-019-57344-4.
Ligi, M., Bonatti, E., Cipriani, A., Ottolini, L., 2005. Water-rich basalts at mid-ocean-ridge cold spots. Nature 434, 66. https://doi.org/10.1038/nature03264.
Ligi, M., Cuffaro, M., Chierici, F., Calafato, A., 2008. Three-dimensional passive mantle flow beneath mid-ocean ridges: an analytical approach. Geophys. J. Int. 175 (2), 783–805. https://doi.org/10.1111/j.1365-246X.2008.03931.x.
Lin, J., Phipps Morgan, J., 1992. The spreading rate dependence of three-dimensional mid-ocean ridge gravity structure. Geophys. Res. Lett. 19 (1), 13–16.
Lizarralde, D., Gaherty, J.B., Collins, J.A., Hirth, G., Kim, S.D., 2004. Spreading-rate dependence of melt extraction at mid-ocean ridges from mantle seismic refraction data. Nature 432 (7018), 744–747.
Lonsdale, P., 1986. Tectonic and magmatic ridges in the Eltanin fault system, South Pacific. Mar. Geophys. Res. 8 (3), 203–242. https://doi.org/10.1007/bf00305484.
Mackwell, S.J., Kohlstedt, D.L., 1990. Diffusion of hydrogen in olivine: implications for water in the mantle. J. Geophys. Res., Solid Earth 95 (B4), 5079–5088.
Martinez, F., Hey, R., 2017. Propagating buoyant mantle upwelling on the Reykjanes Ridge. Earth Planet. Sci. Lett. 457, 10–22. https://doi.org/10.1016/j.epsl.2016.1009.1057.
Martinez, F., Hey, R., Höskuldsson, Á., 2020. Reykjanes Ridge evolution: effects of plate kinematics, small-scale upper mantle convection and a regional mantle gradient. Earth-Sci. Rev. 206. https://doi.org/10.1016/j.earscirev.2019.102956.
Naar, D.F., Hey, R.N., 1989. Speed limit for oceanic transform faults. Geology 17, 420–422.
Phipps Morgan, J., 1997. The generation of a compositional lithosphere by mid-ocean ridge melting and its effect on subsequent off-axis hotspot upwelling and melting. Earth Planet. Sci. Lett. 146, 213–232.
Phipps Morgan, J., Forsyth, D.W., 1988. Three-dimensional flow and temperature perturbations due to a transform offset: effects on oceanic crustal and upper mantle structure. J. Geophys. Res., Solid Earth 93 (B4), 2955–2966.
Plank, T., Langmuir, C.H., 1992. Effects of the melting regime on the composition of the oceanic crust. J. Geophys. Res., Solid Earth 97 (B13), 19749–19770.
Püthe, C., Gerya, T., 2014. Dependence of mid-ocean ridge morphology on spreading rate in numerical 3-D models. Gondwana Res. 25 (1), 270–283. https://doi.org/10.1016/j.gr.2013.04.005.
Sandwell, D.T., Müller, R.D., Smith, W.H.F., Garcia, E., Francis, R., 2014. New global marine gravity model from CryoSat-2 and Jason-1 reveals buried tectonic structure. Science 346 (6205), 65–67. https://doi.org/10.1126/science.1258213.
Schierjott, J.C., Thielmann, M., Rozel, A.B., Golabek, G.J., Gerya, T.V., 2020. Can grain size reduction initiate transform faults?—Insights from a 3-D numerical study. Tectonics 39 (10), e2019TC005793. https://doi.org/10.1029/2019TC005793.
Schmädicke, E., Gose, J., Stalder, R., 2018. Water in abyssal peridotite: why are melt-depleted rocks so water rich? Geochem. Geophys. Geosyst. 19 (6), 1824–1843.
Schouten, H., White, R.S., 1980. Zero-offset fracture zones. Geology 8 (4), 175–179. https://doi.org/10.1130/0091-7613(1980)8<175:zfz>2.0.co;2.
Searle, R.C., Keeton, J.A., Owens, R.B., White, R.S., Mecklenburgh, R., Parsons, B., Lee, S.M., 1998. The Reykjanes Ridge: structure and tectonics of a hot-spot-influenced, slow-spreading ridge, from multibeam bathymetry, gravity and magnetic investigations. Earth Planet. Sci. Lett. 160 (3–4), 463–478.
Shen, Y., Forsyth, D.W., 1992. The effects of temperature- and pressure-dependent viscosity on three-dimensional passive flow of the mantle beneath a ridge-transform system. J. Geophys. Res., Solid Earth 97, 19,717–719,728.
Smallwood, J.R., White, R.S., 2002. Ridge-plume interaction in the North Atlantic and its influence on continental breakup and seafloor spreading. Geol. Soc. (Lond.) Spec. Publ. 197 (1), 15–37. https://doi.org/10.1144/gsl.sp.2002.197.01.02.
Smallwood, J.R., White, R.S., Minshull, T.A., 1995. Sea-floor spreading in the presence of the Iceland plume: the structure of the Reykjanes Ridge at 61°40′N. J. Geol. Soc. 152 (6), 1023–1029. https://doi.org/10.1144/gsl.jgs.1995.152.01.24.
Taylor, B., Goodliffe, A., Martinez, F., 2009. Initiation of transform faults at rifted continental margins. C. R. Géosci. 341 (5), 428–438. https://doi.org/10.1016/j.crte.2008.1008.1010.
Tolstoy, M., Harding, A.J., Orcutt, J.A., 1993. Crustal thickness on the Mid-Atlantic Ridge: bull's-eye gravity anomalies and focused accretion. Science 262, 726.
Turcotte, D.L., 1974. Are transform faults thermal contraction cracks? J. Geophys. Res., Solid Earth 79, 2573–2577.
Vogt, P.R., 1971. Asthenosphere motion recorded by the ocean floor south of Iceland. Earth Planet. Sci. Lett. 13 (1), 153–160.
Wessel, P., Luis, J.F., Uieda, L., Scharroo, R., Wobbe, F., Smith, W.H.F., Tian, D., 2019. The Generic Mapping Tools Version 6. Geochem. Geophys. Geosyst. https://doi.org/10.1029/2019gc008515.
White, R.S., 1997. Rift-plume interaction in the North Atlantic. Philos. Trans. R. Soc., Math. Phys. Eng. Sci. 355 (1723), 319–339.
White, R.S., Bown, J.W., Smallwood, J.R., 1995. The temperature of the Iceland plume and origin of outward-propagating V-shaped ridges. J. Geol. Soc. 152 (6), 1039–1045. https://doi.org/10.1144/gsl.jgs.1995.152.01.26.
Wilson, J.T., 1965. A new class of faults and their bearing on continental drift. Nature 207, 343–347.